Non-stationary statistical modelling of wind speed: A case study in eastern Canada

Taha B.M.J. Ouarda[1,*], Christian Charron[1]

[1]Canada Research Chair in Statistical Hydro-Climatology, Institut national de la recherche scientifique, Centre Eau Terre Environnement, 490 rue de la Couronne, Québec, QC, G1K 9A9, Canada

*Corresponding author
Email: taha.ouarda@ete.inrs.ca
Tel: +1 418 654 3842

October 2020

Abstract:

The assessment of wind energy potential is generally based on the analysis of the statistical distribution of observed wind speed of short time resolution. Record periods of observational data used in practice at sites of interest are often very short, often ranging from a few months to a few years. Predictions based on such small record periods are likely to be biased as it is recognized that wind speed is subject to important interannual variability and long-term trends. Large-scale atmospheric circulation patterns have an important influence on wind speed. Their predictable nature can make them useful for the prediction of wind speed during the lifetime of wind farm projects. This feature is not exploited in practice. It is proposed in this study to introduce predictors of the wind speed in non-stationary statistical models. This approach allows the development of predictions of the wind speed distribution conditionally on the state of the predictors. The predictors used here are indices of atmospheric circulation to account for the interannual variability and a temporal index to account for the long-term temporal trend. The proposed approach was applied to hourly wind speed data at selected meteorological stations in the province of Québec (Canada). 20 stations with long record periods of over 30 years of data were used. The most important circulation indices identified in the study area are the North-Atlantic Oscillation (NAO) during the winter season and the Pacific North American (PNA) during the spring season. Results indicate that the annual goodness-of-fit at the stations of the case study improved on average when the non-stationary model is used compared to the stationary model. The proposed approach can potentially be used to model wind speed during the projected lifetime of wind farms using forecasts of the predictors.

Keywords: Wind speed; Wind Energy; Non-stationary model; Probability density function; Climate oscillation indices; Climate variability.

1. Introduction

For the assessment of wind energy potential and the design of wind farms, knowledge of the probability distribution of wind speed of short time resolution (typically hourly data) at sites of interest is essential. A common practice is to fit a probability density function (pdf) to observed short-term wind speed data (Ouarda et al., 2015). Observational wind speed data at the sites of interest are often not available for long periods and it is common in practical studies to use data for record periods as short as only a few months to a few years (Celik, 2004; Morgan et al., 2011). Considering that the expected lifetime for wind farms is about 30 years (Pryor et al., 2005), this is generally insufficient. Nevertheless, recent advances in meteorological reanalysis products provide the opportunity to use wind data over large areas and for extended periods (Holt and Wang, 2012). Regardless of the available record period of the wind speed data, the classical approach assumes that wind speed characteristics are homogeneous throughout the whole observed period and will also remain constant during the projected life of the wind farm project. However, it is recognized that wind speed is subject to important interannual variability and decadal trends, which have major impacts on the wind power output delivery (Naizghi and Ouarda, 2017).

Several studies analysed trends in wind speed time series around the world from near-surface observed data sets or reanalysis data sets. Studies that have analyzed trends from observational data sets have generally found declines over the last 30–50 years for stations located in mid-latitude (e.g. studies in Australia (McVicar et al., 2008), China (Zhang et al., 2019a) or the United-States (Pryor et al., 2009)). Converse results to those of observational data sets are often obtained with reanalysis data sets and the recent decline in wind speed observed from near surface stations is rarely reflected in the reanalyses (McVicar et al., 2008; Pryor et al., 2009; Holt and Wang, 2012).

In North America, the majority of studies using observational data found spatially coherent and statistically significant decreasing trends. Pryor et al. (2009) analysed trends in historical wind speed over the contiguous United States based on observational and reanalysis data sets. For the observational data sets, the majority of stations exhibit declines in the 50th and 90th percentile wind speeds for the period 1973–2005, and these trends are even stronger over the eastern United States and the Midwest. On the other side, converse trends were obtained in the output of the data sets analysed from different reanalysis products. Holt and Wang (2012) found statistically significant positive annual trends over the contiguous United States using the North American Regional Reanalysis (NARR). In Canada, Wan et al. (2010) used homogenized near-surface wind speed time series from meteorological stations. They found significant decreasing trends throughout western Canada and most parts of southern Canada in all seasons and significant increasing trends in the central Canadian Arctic in all seasons and in the Maritimes in spring and autumn. The dependence of trend on latitude in these results was confirmed by Wang et al. (2006).

A number of causes and explanations of the downward trends in observational data sets have been suggested in the literature. Changes in atmospheric circulation patterns have been identified as having a major influence on wind speed variability (Wang et al. 2006; Hurrell and Deser, 2009). It has also been pointed out that observational wind data are highly inhomogeneous: stations are subject to frequent changes of anemometer type, location or height to which wind observations are sensitive (Wan et al., 2010). Some authors such Vautard et al. (2010) and Zhang et al. (2019b) attributed the decline in wind speed partly to the increase in surface roughness associated with factors such as urbanization, growth of forests, changes in forest distribution or changes in agricultural practices. Zhang et al. (2019b) indicated that atmospheric circulation explains monthly variation in surface wind speed during the past decades, but that the increased surface friction dominates the long-term declining trend of wind speed. For Vautard et al. (2010), the failure of reanalysis models to replicate surface wind trends is due to the non-consideration of land use changes in the reanalyses.

Climate variability in the tropical Atlantic has been largely associated with multiple large-scale atmospheric circulation patterns (Sutton et al., 2000). The North-Atlantic Oscillation (NAO) has been identified as the most prominent mode of variability in the North-Atlantic region. Studies have established that many circulation patterns have important influence on wind speed variability in North America. Wang et al. (2006) found that the cyclone activity in Canada is closely related to the NAO, the Pacific Decadal Oscillation (PDO), and the El Niño–Southern Oscillation (ENSO) indices. Among these indices, the NAO is the index that most explains the cyclone variance. They found that a strong positive NAO is associated with more frequent cyclone activity in the high Arctic and less frequent activity on the east coast in all seasons but most significant during winter. Abhishek et al. (2010) found that the Pacific North America (PNA) index has the highest association with wind speed trends in three cities in the USA Midwest. Klink (2007) showed that wind speed variation is related to the Arctic Oscillation (AO) and the Niño-3.4 sea surface temperature (SST) anomalies.

The most important consequence of the interannual variability and long-term trends in wind speed on wind energy assessment is that predictions may be inaccurate. This is especially true for the record periods that are noticeably short and which are used in the field of wind energy. Pryor et al. (2005) highlighted this problem by showing that using the data from the period of 1987–1998 leads to an overestimation of the wind energy in Denmark relative to the period of 1958–2001 by approximately 10%. The persistent and potentially predictable nature of atmospheric circulation patterns can also be exploited to provide tools for the prediction of wind power output. Classical models used in wind energy assessment do not take into consideration atmospheric circulation patterns and oscillations. Indeed, short term or long-term predictions of large-scale circulation patterns can help predict the future evolution of wind speed and consequently better predict the energy potential during the lifespan of a given wind farm project (Woldesellasse et al., 2020).

A significant number of studies are devoted to the forecasting of short-term wind speed or corresponding wind energy (e.g. Wang et al., 2018). However, very few studies have looked at the prediction of long-term wind speed or wind power. Short-term predictions are generally made over a time horizon of a few hours to a few days, while long-term predictions are made over a time horizon of a few months, years or decades. Some approaches have been proposed to integrate predictors of the wind speed variability in tools for the prediction of long-term wind speed or power. Brayshaw et al. (2011) proposed to use a prediction of the state of NAO (high, medium or low) at some time in the future to obtain a statistical forecast of the power output. At each month of these NAO forecasts, the NAO index is used to generate artificial time-series of wind speed for that month. In Correia et al. (2017) and Jerez and Trigo (2013), circulation modes were used as predictors in multiple linear regression models to assess wind power at the monthly timescale. These latter models, when combined with forecasts of the studied circulation modes, allow to predict the wind power output. Similarly, Garrido-Perez et al. (2020) used a regression model to explain the monthly capacity factor using monthly frequencies of occurrence of weather regimes as predictors.

These approaches somehow diverge from the traditional line in that the distribution of wind speed is not represented with a statistical model. Instead, forecast of a single point value representing the wind power for a given period is obtained. A new approach is proposed here for the prediction of the full wind speed distribution for a given period using its pdf parameters. It consists in introducing covariates into the parameters of the probability distribution used for wind speed modelling. Such covariates could incorporate trends, cycles, physical characteristics or other phenomena that can explain the studied variable. The resulting models, often called non-stationary models, are therefore distribution functions that are conditional on time-dependent covariates. With such model, future wind speed distributions can potentially be obtained using forecasts of the covariates. Forecasts of low frequency climate oscillation indices are available from several climate modeling approaches (see for instance Lee and Ouarda, 2019).

A similar approach is slowly gaining popularity for the incorporation of information concerning non-stationarities in research efforts dealing with the modeling of hydro-meteorological extremes (El Adlouni et al., 2007; Hundecha et al., 2008; Thiombiano et al., 2017; Ouarda et al., 2019). However, this approach has never been adapted and used for the modelling of wind speed in the context of wind energy assessment. In the context of modeling hydro-meteorological extremes, a single extreme value is extracted each year within a season or a year (e.g. spring flood, summer maximum temperature), while in the context of assessment of wind energy, we are interested in the whole distribution of wind speed corresponding to small time scales during a season or a year. The non-stationary approach needs to be adapted to the particular context of the assessment of wind energy where the studied variable is on a time scale of typically one hour. In that context, it is assumed that the predictors or covariates modulate the shape of the distribution of the hourly wind speed on a seasonal or annual basis. The non-stationary statistical model presented here predict the hourly wind speed distribution for a given season or year as a function of the specific state of the covariates.

Numerous studies have dealt with the identification of the appropriate wind speed pdf with the objective of reducing wind power estimation error (Kose et al., 2004; Akpinar and Akpinar, 2005). The Weibull (W) distribution is traditionally the most widely used and accepted probability distribution to model wind speed in the wind energy field (Tuller and Brett, 1985; Archer and Jacobson, 2003; Ouarda et al., 2015). However, more complex models were recently found to provide better fit to wind speed data in several studies (Ouarda et al., 2015). Mixture models of one-component distributions have also been shown to provide excellent fit when a bimodal wind speed behaviour is observed (Wang et al., 2019; Chang, 2011). Ouarda and Charron (2018) evaluated the suitability of a selection of several one-component distributions and two-component mixture distributions to model wind speed data over the same region analysed in the present study. While mixture models provided better fit that the one-component distributions at a number of stations, the W provided a general good fit and was the best one-component distribution with one shape parameter. In the present study, the W distribution is used to illustrate the non-stationary approach (NS-W) for the modeling of hourly wind speed series. The approach presented in the present study should be adapted to other distribution functions and to mixture models in future research efforts.

The proposed approach is illustrated here on a case study in southern Québec (Canada) for 20 stations with long time series of observed hourly wind speed data. This study is site specific and identifies the atmospheric circulation indices having the most influence on wind speed distribution in the study area, to be used as covariates in the non-stationary approach. An index of time is also used as covariate to account for long-term temporal trends. This study is focused on the extended winter season (December to May) as it is during that season that the circulation patterns have the biggest impacts on wind speed and it is also the period with the strongest winds in the study area.

2. Methodology

An overview of the proposed methodology for wind energy assessment at a given site of interest over a long-term horizon is presented in Figure 1. The main steps are as follows:

1. Selection of covariates such as climate oscillation indices. Trend detection is usually carried out on wind speed time series to assess the appropriateness of including the temporal trend as a covariate.
2. Selection of the most suitable non-stationary model for observed wind speed data (e.g. the non-stationary Weibull pdf).
3. Fitting of the non-stationary model and estimation of model parameters.
4. Forecast of the covariates for the period of interest.
5. Forecast of long-term future wind speed distributions on a seasonal or annual basis.
6. Long-term prediction of wind power.

2.1 Non-stationary Weibull distribution

The NS-W model is used in this study to model hourly wind speed where the distribution parameters are modulated by a linear combination of one or several covariates. The cumulative distribution function (cdf) of the stationary W model is given by:

$$F\left(x;\alpha,k\right)=1-\exp\left[-\left(\frac{x}{\alpha}\right)^{k}\right] \tag{1}$$

where $x>0$ is the wind speed, $\alpha>0$ is a scale parameter and k is a shape parameter. $F(x)$ represents the distribution of the hourly wind speed during the whole record period. In the non-stationary framework, the parameters of $F(x)$ are made linearly dependent upon one or several time-varying covariates. The conditional cdf of the NS-W model is then given by:

$$F\left(x;\alpha_t,k_t\right)=1-\exp\left[-\left(\frac{x}{\alpha_t}\right)^{k_t}\right] \tag{2}$$

where t represents increments in the defined time step. In the case of a dependence on the covariate X_t, we have:

$$\alpha_t=\alpha_0+\alpha_1 X_t \text{ and } k_t=k_0+k_1 X_t. \tag{3}$$

In the case of a dependence on both covariates X_t and Y_t, we have:

$$\alpha_t=\alpha_0+\alpha_1 X_t+\alpha_2 Y_t \text{ and } k_t=k_0+k_1 X_t+k_2 Y_t. \tag{4}$$

Therefore, $F\left(x;\alpha_t,k_t\right)$ represents the distribution of the hourly wind speed data during the tth season or year, conditional on the values of the covariates X_t and Y_t associated with that season or year.

2.2 Parameter estimation

The parameters of the models are estimated here with the least-squares (LS) method which is commonly used for the modelling of wind speed data (Carta and Ramirez, 2007; Shin et al., 2016; Jung and Schindler, 2017). For that, the observed wind speed data is arrangement into N class intervals $[0,v_1),[v_1,v_2),...,[v_{N-1},v_N]$. The relative frequency at the ith class interval is given by $p_i=F(v_i)-F(v_{i-1})$ where v_{i-1} and v_i are the lower and upper limits of the ith class interval and the cumulative empirical probability at the ith class is obtained by $P_i=\sum_{j=1}^{i}p_j$. In the stationary framework, the objective function, which is the sum squared errors (SSE) for the LS method, is defined by:

$$\mathrm{SSE} = \sum_{i=1}^{N} \left[P_i - F(v_i; \alpha, k) \right]^2 \tag{5}$$

where v_i is the upper limit of the ith class interval.

In the non-stationary framework, each year is considered separately and the SSE is computed for each year. The objective function is then defined by the mean value of the individual SSEs:

$$\mathrm{SSE} = \frac{1}{n_{yr}} \sum_{j=1}^{n_{yr}} \sum_{i=1}^{N_j} \left[P_{i,j} - F(v_{i,j}; \alpha_j, k_j) \right]^2 \tag{6}$$

where n_{yr} is the number of years, N_j is the number of class intervals for the jth year, $v_{i,j}$ is the upper limit of the ith class interval for the jth year, $P_{i,j}$ is the cumulative empirical probability at the ith class interval for the jth year, and α_j and k_j are the values of the parameters for the jth year. Equations 5 and 6 can be solved with any numerical optimization tool. α and k are the parameters to estimate for the stationary model, $\alpha_0, \alpha_1, k_0, k_1$ are the parameters to estimate for the non-stationary model with one covariate and $\alpha_0, \alpha_1, \alpha_2, k_0, k_1, k_2$ are the parameters to estimate for the non-stationary model with two covariates. Equations 5 and 6 are solved here with the optimization function *fminsearch* in the MATLAB environment (MATLAB, 2019).

2.3. Model validation

In addition to the SSE computed during the optimization step, other statistics such as the Akaïke information criterion (AIC), the chi-square test statistic (χ^2), the coefficient of determination (R^2) and the Kolmogorov-Smirnov test statistic (KS) are used for the validation of the goodness-of-fit of the various models. These criteria are frequently used for the evaluation of the goodness-of-fit in the field of wind energy (Ouarda et al., 2016). To compute these statistics, wind speed data are arranged in the same N class intervals defined in the model parameters estimation step. For the non-stationary models, these statistics are computed yearly and the global statistics are obtained by the mean values.

The AIC accounts for goodness-of-fit and has the advantage of penalizing for model complexity (number of parameters). It is given by:

$$\mathrm{AIC} = -2\log(L(\hat{\theta})) + 2d \tag{7}$$

where $L(\hat{\theta})$ is the likelihood function for the estimated model distribution parameters $\hat{\theta}$, and d is the number of parameters in the model. R^2 gives the proportion of the variance of the observed data that is explained by the model. Two different indices to compute R^2 are used here. The first one is defined by:

$$R_F^2 = 1 - \frac{\sum_{i=1}^{N}(P_i - \hat{F}_i)^2}{\sum_{i=1}^{N}(P_i - \bar{P})^2} \tag{8}$$

where $\hat{F}_i$ is the predicted value of $F(v_i)$ at the ith class interval and $\bar{P}$ is the mean value of P_i. The second one is defined by:

$$R_p^2 = 1 - \frac{\sum_{i=1}^{N}(p_i - \hat{p}_i)^2}{\sum_{i=1}^{N}(p_i - \bar{p})^2} \tag{9}$$

where $\hat{p}_i$ is the estimated probability at the ith class interval and $\bar{p}$ is the mean value of p_i. The R^2 indices are further adjusted to account for models complexity with the following formula:

$$R_{adj}^2 = 1 - (1 - R^2)\frac{n-1}{n-p} \tag{10}$$

The χ^2 test statistic is a measure the adequacy of a given theoretical distribution to a data sample and is expressed as:

$$\chi^2 = \sum_{i=1}^{N} \frac{(O_i - E_i)^2}{E_i} \tag{11}$$

where O_i is the observed frequency in the *i*th class interval and E_i is the expected frequency in the *i*th class interval. When E_i for a given class interval is very small, it is combined with the adjacent class interval in order to avoid the situation where E_i has an excessive weight. Finally, the KS statistic corresponds to the largest difference between the predicted and the observed distribution and is given by:

$$KS = \max_{1 \le i \le N} \left| P_i - \hat{F}_i \right|. \tag{12}$$

A lower value of AIC, χ^2, SSE or KS, and a higher value of R^2 indicate a better fit.

3. Data

The wind speed data used in this study were obtained from the Environment and Climate Change Canada's (ECCC) historical climate database (available at http://climate.weather.gc.ca). ECCC indicates that the vast majority of observational data is accurate, but the database may exceptionally contain some individual incorrect values. ECCC continues to review quality control procedures, both as current data is observed and incorporated into the database, and retrospectively for historical data. Wind speed data consist of hourly mean wind speeds observed at meteorological stations 10 m above the ground. The stations for this study area were selected exclusively from the province of Quebec (Canada). The same region was studied in Ouarda and Charron (2018) to explore the potential improvement in fitting wind speed data by using homogeneous and heterogeneous mixtures of distributions in a stationary environment. In this database, it is frequent for stations to be renamed (station number) or moved. Whenever possible, stations were combined to increase the record length of the times series at a given location. For that, stations with the same coordinates or located at very close distances from each other and at a similar altitude have been combined together.

Among the candidate stations, those with a record length of at least 30 years and located in the southern part of the province (below latitude 55°N) were considered. In all, 20 stations were selected for this study. The geographical location of the selected stations is presented in Figure 2. Several stations are located on both sides of the Saint-Lawrence River estuary in the southern part of the province. Table 1 presents information concerning the period of record and the geographical location of each station in the present study.

Plots of average monthly wind speed at the meteorological stations reveal that the months from November to April are in general the windiest for the region of study. It can be observed that there is a different seasonality between the northwestern stations (stations #1 to #5 and #15) and the southern stations along the Saint-Lawrence River. The seasonality of the northwestern stations is characterised by an extended windy season with two distinct monthly periods of highest speeds occurring in spring and autumn, while the stations along the Saint-Lawrence River are characterised by a shorter windy period occurring during the winter season in which the highest wind speeds take place. Figure 3 illustrates the average monthly wind speed at the stations of

Montréal/St-Hubert and Val-d'Or, representing respectively the seasonality of the southern and northwestern stations.

Monthly data of the major climate indices having impacts in North America were obtained from the NOAA Physical Sciences Laboratory data base available at https://psl.noaa.gov/data/climateindices/list/. Data are available as monthly time series and are updated regularly. In this study, the following climate indices were considered: the PDO, the PNA, the NAO, the AO, the Atlantic Multi-decadal Oscillation (AMO), the southern oscillation index (SOI), and the Western Hemisphere Warm Pool (WHWP). Times series for most of these indices are available from 1950 to present.

4. Results and discussions

4.1. Relation with atmospheric circulation patterns and trends

In this study, the identification of the seasonal atmospheric circulation indices having the most impact on seasonal wind speed is carried out by means of the correlations between the selected seasonal climate indices and the seasonal wind speed averages. For this, the correlation coefficients between the average of a given index over 3 consecutive months and the average wind speed over the same period are computed. Results show that NAO and PNA have a dominant influence in the region. Figure 4 presents the boxplots of the correlation coefficients obtained at all stations for the NAO and PNA indices. These graphs show that NAO during the winter season and PNA during the spring season have the most influence. This is consistent with the literature where NAO and PNA were identified as major circulation modes in the extratropical Northern Hemisphere (Hurrell and Deser, 2009).

It can be observed that the strongest relation exists during the season of December, January and February (DJF) for NAO, and during the season of March, April, and May (MAM) for PNA. The selected covariates are thus denoted by NAO (DJF) and PNA (MAM). The boxplot for NAO during the DJF season indicates that most of the correlations are significant and shows the presence of some significant positive correlations. It was decided here to study the DJF and MAM seasons separately because of the successive preponderant influence of NAO and PNA. It was also decided to study the whole DJFMAM season because it is the period with the strongest wind speeds in general in the study area and the two selected climate indices have influences during this period.

Table 2 presents the correlation coefficients between the annual mean wind speed during each season of interest and the selected seasonal climate indices. The correlations with a temporal index (denoted Time), which represent the temporal trend, are also presented. Significant correlations at a confidence level of 10% using the student *t*-test are highlighted. For both climate indices, most correlations are significant and more significant correlations are observed for NAO during the DJF season and for PNA during the MAM season. Results show that the sign of the correlation for NAO is mostly negative but there are also few positive correlations. These positive correlations occur mainly for the stations located in the northwestern part of the study area. This indicates a possible spatial discontinuity in the influence of NAO. It is difficult to conclude here as the northwestern area is spatially not well represented by the meteorological stations. An opposite effect of NAO on the climate of northeastern America is well documented in several studies (Kingston et al., 2006a, 2006b; Hurrell, 1995). In the case of PNA, all correlations are negative and most are significant. This is consistent with previous studies on the impact of PNA on hydro-climatic variables in northeastern America (see for instance Thiombiano et al., 2018).

Several significant decreasing trends are observed in the time series. The stations with no significant trend or with positive trends are a mixture of stations within the northwestern region (stations #1 to #5) and stations with a more recent record period (1981 and after) (stations #5 and #18-19). This last observation may indicate a climate change signal in the studied area during the last 30 years. Figure 5 presents the temporal long-term trends in the selected seasonal climate indices used as covariates. It can be observed that there is a constant increase in NAO (DJF) during the studied period. For PNA (MAM), the linear trends from 1952 to 1982 and from 1983 to 2020 are presented to highlight an apparent change in the trend around the mid-1980s. The year of 1983 was chosen as an approximative starting date for the stations with more recent starting dates in the 1980s. A part of the negative trend in the wind speed time series may possibly be attributed to the increasing trend in NAO (DJF) since the 1950s. On the other hand, the increasing trends in stations with a more recent record (starting date) may be due to the negative trend in PNA (MAM) since 1983.

Figures 6-7 illustrate the possible impacts of the climate indices on the shape of the wind speed distribution. Figure 6 presents the frequency histograms along the fitted W model for the observed wind speed data at selected stations where data are divided according to the positive phase and negative phase of a given climate index. Figures 6a-b present wind speeds for the winter season (DJF) classified according to the positive and negative phases of NAO (DJF) at the stations of Mont-Joli and Québec/Jean Lesage Intl., and Figures 6c-d present wind speeds for the spring season (MAM) classified according to the positive and negative phases of PNA (MAM) at the stations of Bagotville and Val-D'Or.

Figure 7 presents the pdf curves of the fitted W model for the observed wind speed data at the stations of Bagotville and Québec/Jean Lesage Intl. during the winter-spring season

(DJFMAM) where data are classified according to the positive and negative phases of NAO (DJF) and PNA (MAM). These figures show that atmospheric circulation patterns can have a strong influence on the inter-annual variability of the shape of the wind speed distribution and show that a model that is conditional on predictors can improve the inter-annual estimates.

4.2 Performances of non-stationary statistical models

The NS-W model was fitted to the wind speed time series of the case study. For the DJFMAM season, models with the covariates Time, NAO (DJF), PNA (MAM), Time and NAO (DJF), Time and PNA (MAM), NAO (DJF) and PNA (MAM) were used (denoted respectively as Time, NAO, PNA, Time+NAO, Time+PNA and NAO+PNA). For the DJF season, models with the covariates Time, NAO (DJF), Time and NAO (DJF) were used (denoted respectively as Time, NAO, Time+NAO). For the MAM season, models with the covariates Time, PNA (MAM), Time and PNA (MAM) were used (denoted respectively as Time, PNA and Time+PNA).

The stationary W model is also fitted to the wind speed time series for comparison purposes. The performances of the models are evaluated and compared here with the different goodness-of-fit indices. Goodness-of-fit statistics for all the stations are presented with boxplots in Figures 8-10 for the DJFMAM, DJF and MAM season respectively. Table 3 presents the parameters and the statistics SSE (see equation 6) and R_F^2 obtained for the DJFMAM season and for selected stations.

All the non-stationary models improve the goodness-of-fit with respect to the stationary model. The model Time provides in general better performances than models including a single climate index or two climate indices in the case of the DJFMAM season. Results show that models including the temporal index and a climate index give the overall best performances for any season. It can be concluded that the temporal trend is an important component of the wind speed variability, and it is only partly explained by the climate indices. Consequently, the temporal index explains to a large extent the long-term wind speed trend (change signal), while climate indices explain partly the interannual variability.

The parameter coefficients of the NS-W models including Time in Table 3 show that a downward trend (most negative signs) is generally observed at the stations of the case study. Possible causes to explain the observed downward trends during the last decades have been discussed in the introduction. A portion of the observed wind speed trend may be attributed to changes in climate indices, as trends were noticed in the seasonal climate indices (see Figure 5). Since Time leads to a better performance than a single climate index or the use of two climate indices, trends in the climate indices cannot represent the only explanation. The increase in surface friction has been pointed out in a number of publications as a possible cause for the generally observed decreasing trends (Vautard et al., 2010; Zhang et al., 2019b). Most meteorological stations of this study are located in airports, and consequently are often located near cities or urban developments, which may have undergone a number of urban changes. This may possibly explain that stations in the northwest, a remote pristine area with low population density, did not observe decreasing trends.

With non-stationary models, the shape of the distribution depends upon the state of the covariates. Figure 11 illustrates the different probability density functions predicted by the model Time+NAO for the DJF season at the station Québec/Jean Lesage Intl. For each year, the distribution of the wind speed with the value of NAO (DJF) for that year is displayed. It can be observed that a large range of different shapes of the distribution are obtained. This additional information detail can have a number of practical uses in the wind energy field. For instance, since the magnitudes of low frequency climate oscillation indices can be forecasted for several seasons and years into the future, the information discussed above can be used to schedule maintenance activities during years and periods of low wind speeds. This would lead to a reduction of the impact of these scheduled maintenance activities on wind energy production.

5. Conclusions and future work

In this study, it was shown that modelling wind speed distributions for the aim of energy assessment without considering the inter-annual variability or long-term trend can lead to important biases in the predictions. This is especially true in the field of wind energy where modelling is usually based on relatively short record periods. It was proposed in this work to introduce predictors of wind speed as covariates in a non-stationary statistical model. Covariates used here are indices of atmospheric circulation patterns to account for the inter-annual variability and a temporal index to account for the long-term temporal trend.

This approach has allowed to better model the observed wind speed series of the case study. It can also potentially provide a tool to predict wind energy potential during the future lifetime of wind farms. By using available short-term or long-term forecasts of the atmospheric circulation indices and other predictors, this model has the potential to provide valuable future predictions of wind speeds. The proposed approach has the advantage, over other approaches, of modeling the shape of the distribution as a function of the covariates instead of only the value of a given wind statistic. Instead of having a one-time estimate of the potential of a wind farm, the approach presented in this work allows to look at the annual evolution of the energy potential of the farm, and may affect the economic feasibility of the whole project, or even the decision about the starting date of the project. This is especially true for projects in which some sort of long-term energy storage is considered (see Loutatidou et al., 2017 for instance). Future efforts should also focus on the development of approaches to carry out sensitivity analysis for the proposed non-stationary models for wind resource assessment (see Tsvetkova and Ouarda, 2019 for instance), and on the comparative modeling of the uncertainty associated to stationary and non-stationary wind speed models. Future research efforts should also look into the development of non-stationary mixed distribution models, as mixed distributions were shown in a number of studies to lead to a better fit than one-component models. The non-stationary approach should also be adapted to statistical distributions other than the Weibull, since previous studies have shown that different models lead to the best fit in different geographical regions. All these efforts should lead to better estimates of the wind speed distribution, and to an improved assessment of the true wind energy potential in different geographical regions.

The most important atmospheric circulation patterns that influence wind speeds in the study region were identified by the mean of correlations. It was found that NAO during the winter season and PNA during the spring season have the most impact on the wind speed distribution. The selected seasonal climate indices were introduced in a non-stationary Weibull model. Results showed that the annual goodness-of-fit was significantly increased on average with the non-stationary models compared to the stationary one.

Results showed that the temporal trend, when it exists, is an important factor to explain long-term wind speed. The climate indices may partly explain the observed trends. For instance, the winter NAO index has constantly increased since the 1950s. However, results showed that climate indices alone do not explain all the long-term trend but may explain the interannual variability.

Other factors may have also influenced the observed wind speeds in the study region. Surface friction related to urbanization near the meteorological stations may also have had an influence on wind speed distribution. It is important to mention that any relevant covariate can be introduced in the model including an index of urbanisation, a roughness or friction coefficient, etc. Covariates of interest may represent natural or anthropogenic influences. The use of other relevant predictors should be considered in the proposed approach in future studies.

Homogenization of data in Canada was performed in other studies such as Wan et al. (2010). It is a process that requires extra work and was not performed here. The objective of this study was to illustrate a new method in the field of wind energy. Additional efforts for the homogenization of wind data should be considered in future studies. It would also be interesting to use reanalysis data sets that combine models with observational data. They provide data on a fine spatial grid and are independent of the various measurement instruments used. In addition, trends have been traditionally observed with these reanalysis data in opposite directions to those obtained with observational data. In this study, the LS method was used. Other methods, such as the maximum likelihood method used with success with wind speed data in a number of studies, can be used and may potentially improve the fit of non-stationary models. Future research efforts should develop other methods than LS for the non-stationary modelling of hourly wind speed data.

Acknowledgements

The authors thank the Natural Sciences and Engineering Research Council of Canada (NSERC) and the Canada Research Chairs Program for funding this research. The authors wish to thank Environment and Climate Change Canada for having supplied the wind speed data used in this study. The authors wish to express their appreciation to Dr. Mohamed Al-Nimr, Editor in Chief, Dr. Nesreen Ghaddar, Editor, and three anonymous reviewers for their invaluable comments and suggestions which helped considerably improve the quality of the paper.

Data Availability

Datasets related to this article can be found at http://dx.doi.org/10.17632/kydc3zw9jb.1, an open-source online data repository hosted at Mendeley Data (Charron, 2021).

References

Abhishek, A., Lee, J.-Y., Keener, T.C., Yang, Y.J., 2010. Long-Term Wind Speed Variations for Three Midwestern U.S. Cities. Journal of the Air & Waste Management Association, 60(9): 1057-1064. doi:10.3155/1047-3289.60.9.1057.

Akpinar, E.K., Akpinar, S., 2005. A statistical analysis of wind speed data used in installation of wind energy conversion systems. Energy Conversion and Management, 46(4): 515-532. doi:10.1016/j.enconman.2004.05.002.

Archer, C.L., Jacobson, M.Z., 2003. Spatial and temporal distributions of U.S. winds and wind power at 80 m derived from measurements. Journal of Geophysical Research: Atmospheres, 108(D9): 4289. doi:10.1029/2002jd002076.

Brayshaw, D.J., Troccoli, A., Fordham, R., Methven, J., 2011. The impact of large scale atmospheric circulation patterns on wind power generation and its potential predictability: A case study over the UK. Renewable Energy, 36(8): 2087-2096. doi:10.1016/j.renene.2011.01.025.

Carta, J.A., Ramírez, P., 2007. Use of finite mixture distribution models in the analysis of wind energy in the Canarian Archipelago. Energy Conversion and Management, 48(1): 281-291. doi:10.1016/j.enconman.2006.04.004.

Celik, A.N., 2004. On the distributional parameters used in assessment of the suitability of wind speed probability density functions. Energy Conversion and Management, 45(11-12): 1735-1747. doi:10.1016/j.enconman.2003.09.027.

Chang, T.P., 2011. Estimation of wind energy potential using different probability density functions. Applied Energy, 88(5): 1848-1856. doi:10.1016/j.apenergy.2010.11.010.

Correia, J.M., Bastos, A., Brito, M.C., Trigo, R.M., 2017. The influence of the main large-scale circulation patterns on wind power production in Portugal. Renewable Energy, 102: 214-223. doi:10.1016/j.renene.2016.10.002.

El Adlouni, S., Ouarda, T.B.M.J., Zhang, X., Roy, R., Bobee, B., 2007. Generalized maximum likelihood estimators for the nonstationary generalized extreme value model. Water Resources Research, 43(3): W03410. doi:10.1029/2005WR004545.

Garrido-Perez, J.M., Ordóñez, C., Barriopedro, D., García-Herrera, R., Paredes, D., 2020. Impact of weather regimes on wind power variability in western Europe. Applied Energy, 264: 114731. doi:10.1016/j.apenergy.2020.114731.

Holt, E., Wang, J., 2012. Trends in Wind Speed at Wind Turbine Height of 80 m over the Contiguous United States Using the North American Regional Reanalysis (NARR). Journal of Applied Meteorology and Climatology, 51(12): 2188-2202. doi:10.1175/JAMC-D-11-0205.1.

Hundecha, Y., St-Hilaire, A., Ouarda, T.B.M.J., El Adlouni, S., Gachon, P., 2008. A Nonstationary Extreme Value Analysis for the Assessment of Changes in Extreme Annual Wind Speed over the Gulf of St. Lawrence, Canada. Journal of Applied Meteorology and Climatology, 47(11): 2745-2759. doi:10.1175/2008jamc1665.1.

Hurrell, J.W., 1995. Decadal Trends in the North Atlantic Oscillation: Regional Temperatures and Precipitation. Science, 269(5224): 676. doi:10.1126/science.269.5224.676.

Hurrell, J.W., Deser, C., 2009. North Atlantic climate variability: The role of the North Atlantic Oscillation. Journal of Marine Systems, 78(1): 28-41. doi:10.1016/j.jmarsys.2008.11.026.

Jerez, S., Trigo, R.M., 2013. Time-scale and extent at which large-scale circulation modes determine the wind and solar potential in the Iberian Peninsula. Environmental Research Letters, 8(4): 044035. doi:10.1088/1748-9326/8/4/044035.

Jung, C., Schindler, D., 2019. Wind speed distribution selection – A review of recent development and progress. Renewable and Sustainable Energy Reviews, 114: 109290. doi:10.1016/j.rser.2019.109290.

Kingston, D.G., Lawler, D.M., McGregor, G.R., 2006. Linkages between atmospheric circulation, climate and streamflow in the northern North Atlantic: research prospects. Progress in Physical Geography: Earth and Environment, 30(2): 143-174. doi:10.1191/0309133306pp471ra.

Kingston, D.G., McGregor, G.R., Hannah, D.M., Lawler, D.M., 2006. River flow teleconnections across the northern North Atlantic region. Geophysical Research Letters, 33(14). doi:10.1029/2006GL026574.

Klink, K., 2007. Atmospheric Circulation Effects on Wind Speed Variability at Turbine Height. Journal of Applied Meteorology and Climatology, 46(4): 445-456. doi:10.1175/JAM2466.1.

Kose, R., Ozgur, M.A., Erbas, O., Tugcu, A., 2004. The analysis of wind data and wind energy potential in Kutahya, Turkey. Renewable and Sustainable Energy Reviews, 8(3): 277-288. doi:10.1016/j.rser.2003.11.003.

Lee, T., Ouarda, T.B.M.J., 2019. Multivariate Nonstationary Oscillation Simulation of Climate Indices with Empirical Mode Decomposition. Water Resources Research, 55(6): 5033-5052. doi:10.1029/2018wr023892.

Loutatidou, S., Liosis, N., Pohl, R., Ouarda, T.B.M.J., Arafat, H.A., 2017. Wind-powered desalination for strategic water storage: Techno-economic assessment of concept. Desalination, 408: 36-51. doi:10.1016/j.desal.2017.01.002.

MATLAB. (2019) Version 9.7.0 (R2019b). Natick, MA: The MathWorks Inc.

McVicar, T.R., Van Niel, T.G., Li, L.T., Roderick, M.L., Rayner, D.P., Ricciardulli, L., Donohue, R.J., 2008. Wind speed climatology and trends for Australia, 1975–2006: Capturing the stilling phenomenon and comparison with near-surface reanalysis output. Geophysical Research Letters, 35(20). doi:10.1029/2008GL035627.

Morgan, E.C., Lackner, M., Vogel, R.M., Baise, L.G., 2011. Probability distributions for offshore wind speeds. Energy Conversion and Management, 52(1): 15-26. doi:10.1016/j.enconman.2010.06.015.

Naizghi, M.S., Ouarda, T.B.M.J., 2017. Teleconnections and analysis of long-term wind speed variability in the UAE. International Journal of Climatology, 37(1): 230-248. doi:10.1002/joc.4700.

Ouarda, T.B.M.J., Charron, C., 2018. On the mixture of wind speed distribution in a Nordic region. Energy Conversion and Management, 174: 33-44. doi:10.1016/j.enconman.2018.08.007.

Ouarda, T.B.M.J., Charron, C., Chebana, F., 2016. Review of criteria for the selection of probability distributions for wind speed data and introduction of the moment and L-moment ratio diagram methods, with a case study. Energy Conversion and Management, 124: 247-265. doi:10.1016/j.enconman.2016.07.012.

Ouarda, T.B.M.J., Charron, C., Kumar, K.N., Phanikumar, D.V., Molini, A., Basha, G., 2019. Nonstationary warm spell frequency analysis integrating climate variability and change with application to the Middle East. Climate Dynamics, 53(9-10): 5329-5347. doi:10.1007/s00382-019-04866-2.

Ouarda, T.B.M.J., Charron, C., Shin, J.Y., Marpu, P.R., Al-Mandoos, A.H., Al-Tamimi, M.H., Ghedira, H., Al Hosary, T.N., 2015. Probability distributions of wind speed in the UAE. Energy Conversion and Management, 93: 414-434. doi:10.1016/j.enconman.2015.01.036.

Pryor, S.C., Barthelmie, R.J., Schoof, J.T., 2005. The impact of non-stationarities in the climate system on the definition of ‘a normal wind year’: a case study from the Baltic. International Journal of Climatology, 25(6): 735-752. doi:10.1002/joc.1151.

Pryor, S.C., Barthelmie, R.J., Young, D.T., Takle, E.S., Arritt, R.W., Flory, D., Gutowski, W.J., Nunes, A., Roads, J., 2009. Wind speed trends over the contiguous United States. Journal of Geophysical Research-Atmospheres, 114. doi:10.1029/2008jd011416.

Shin, J.-Y., Ouarda, T.B.M.J., Lee, T., 2016. Heterogeneous mixture distributions for modeling wind speed, application to the UAE. Renewable Energy, 91: 40-52. doi:10.1016/j.renene.2016.01.041.

Sutton, R.T., Jewson, S.P., Rowell, D.P., 2000. The Elements of Climate Variability in the Tropical Atlantic Region. Journal of Climate, 13(18): 3261-3284. doi:10.1175/1520-0442(2000)013<3261:teocvi>2.0.co;2.

Thiombiano, A.N., El Adlouni, S., St-Hilaire, A., Ouarda, T.B.M.J., El-Jabi, N., 2017. Nonstationary frequency analysis of extreme daily precipitation amounts in Southeastern Canada using a peaks-over-threshold approach. Theoretical and Applied Climatology, 129(1-2): 413-426. doi:10.1007/s00704-016-1789-7.

Thiombiano, A.N., St-Hilaire, A., El Adlouni, S.-E., Ouarda, T.B.M.J., 2018. Nonlinear response of precipitation to climate indices using a non-stationary Poisson-generalized Pareto model: case study of southeastern Canada. International Journal of Climatology, 38(S1): e875-e888. doi:10.1002/joc.5415.

Tsvetkova, O., Ouarda, T.B.M.J., 2019. Quasi-Monte Carlo technique in global sensitivity analysis of wind resource assessment with a study on UAE. Journal of Renewable and Sustainable Energy, 11(5): 053303. doi:10.1063/1.5120035.

Tuller, S.E., Brett, A.C., 1985. The goodness of fit of the Weilbull and Rayleigh distribution to the distributions of observed wind speeds in a topographically diverse area. Journal of climatology, 5: 74-94.

Vautard, R., Cattiaux, J., Yiou, P., Thépaut, J.-N., Ciais, P., 2010. Northern Hemisphere atmospheric stilling partly attributed to an increase in surface roughness. Nature Geoscience, 3(11): 756-761. doi:10.1038/ngeo979.

Wan, H., Wang, X.L., Swail, V.R., 2010. Homogenization and Trend Analysis of Canadian Near-Surface Wind Speeds. Journal of Climate, 23(5): 1209-1225. doi:10.1175/2009JCLI3200.1.

Wang, L., Li, X., Bai, Y., 2018. Short-term wind speed prediction using an extreme learning machine model with error correction. Energy Conversion and Management, 162: 239-250. doi:10.1016/j.enconman.2018.02.015.

Wang, X.L., Wan, H., Swail, V.R., 2006. Observed Changes in Cyclone Activity in Canada and Their Relationships to Major Circulation Regimes. Journal of Climate, 19(6): 896-915. doi:10.1175/JCLI3664.1.

Wang, Q., Luo, K., Yuan, R., Zhang, S., Fan, J., 2019. Wake and performance interference between adjacent wind farms: Case study of Xinjiang in China by means of mesoscale simulations. Energy, 166: 1168-1180. doi:10.1016/j.energy.2018.10.111.

Woldesellasse, H., Marpu, P.R., Ouarda, T.B.M.J., 2020. Long-term forecasting of wind speed in the UAE using nonlinear canonical correlation analysis (NLCCA). Arabian Journal of Geosciences, 13(18): 962. doi:10.1007/s12517-020-05981-9.

Zhang, R., Zhang, S., Luo, J., Han, Y., Zhang, J., 2019a. Analysis of near-surface wind speed change in China during 1958–2015. Theoretical and Applied Climatology, 137(3): 2785-2801. doi:10.1007/s00704-019-02769-0.

Zhang, Z., Wang, K., Chen, D., Li, J., Dickinson, R., 2019b. Increase in Surface Friction Dominates the Observed Surface Wind Speed Decline during 1973–2014 in the Northern Hemisphere Lands. Journal of Climate, 32(21): 7421-7435. doi:10.1175/JCLI-D-18-0691.1.

Table 1. List of meteorological stations.

#	Station name	Record period	Latitude	Longitude	Calm (%)	Median (m/s)	CV	Skewness	Kurtosis
1	Rouyn-Noranda	1975 – 2020	48.21	-78.84	7.89	3.06	0.63	0.42	2.93
2	Matagami	1974 – 2020	49.76	-77.80	7.41	3.06	0.63	0.59	3.27
3	Val-D'Or	1955 – 2020	48.06	-77.79	6.05	3.06	0.61	0.61	3.37
4	La Grande Rivière	1978 – 2020	53.63	-77.70	2.93	3.89	0.54	0.69	3.78
5	Chibougamau-Chapais	1983 – 2020	49.77	-74.53	4.67	3.06	0.59	0.57	3.26
6	Montréal Mirabel Intl	1976 – 2020	45.68	-74.04	7.70	2.50	0.69	1.02	4.64
7	Montréal/Pierre Elliott Trudeau Intl	1953 – 2020	45.47	-73.75	4.12	3.61	0.62	0.83	3.95
8	Montréal/St-Hubert	1953 – 2020	45.52	-73.42	6.18	4.17	0.63	0.73	3.75
9	Roberval	1958 – 2020	48.52	-72.27	7.39	3.61	0.65	0.69	3.49
10	Sherbrooke	1963 – 2020	45.44	-71.69	12.76	2.22	0.77	0.96	3.91
11	Québec/Jean Lesage Intl	1953 – 2020	46.79	-71.39	7.93	3.61	0.68	0.71	3.49
12	Bagotville	1953 – 2020	48.33	-71.00	7.74	3.61	0.68	0.69	3.24
13	Mont-Joli	1953 – 2020	48.60	-68.22	3.69	4.72	0.59	0.66	3.40
14	Baie-Comeau	1965 – 2020	49.13	-68.20	3.97	3.89	0.62	0.83	3.93
15	Schefferville	1953 – 2020	54.81	-66.81	5.65	4.17	0.62	0.64	3.55
16	Sept-Iles	1953 – 2020	50.22	-66.27	7.39	3.89	0.67	0.93	4.46
17	Gaspé	1975 – 2020	48.78	-64.48	13.03	2.78	0.78	0.81	3.68
18	Havre-Saint-Pierre	1984 – 2020	50.28	-63.60	4.54	3.61	0.62	0.90	4.18
19	Natashquan	1981 – 2020	50.19	-61.79	2.06	4.17	0.62	1.01	4.53
20	Lourdes-de-Blanc-Sablon	1983 – 2020	51.45	-57.18	4.80	4.72	0.73	1.02	4.16

Table 2. Correlation coefficients between the average wind speed during each season of interest and the selected covariates.

	DJFMAM season			DJF season		MAM season	
#	Time	NAO (DJF)	PNA (MAM)	Time	NAO (DJF)	Time	PNA (MAM)
1	**0.27**	**0.30**	**-0.27**	**0.37**	**0.26**	0.14	**-0.30**
2	**0.50**	**0.32**	**-0.26**	**0.55**	0.25	**0.37**	**-0.27**
3	**0.26**	0.03	-0.19	0.13	0.05	**0.27**	**-0.29**
4	**0.41**	**0.27**	**-0.37**	**0.33**	**0.42**	**0.32**	**-0.37**
5	**0.66**	**0.43**	-0.21	**0.54**	**0.44**	**0.61**	-0.20
6	**-0.70**	-0.19	-0.05	**-0.73**	**-0.27**	**-0.53**	-0.11
7	-0.05	-0.09	**-0.33**	-0.11	-0.15	0.01	**-0.35**
8	**-0.23**	**-0.25**	**-0.26**	**-0.22**	**-0.25**	**-0.21**	**-0.33**
9	**-0.37**	**-0.45**	-0.17	**-0.31**	**-0.42**	**-0.36**	**-0.27**
10	0.08	-0.15	**-0.45**	0.01	**-0.22**	0.14	**-0.45**
11	**-0.52**	**-0.53**	**-0.30**	**-0.46**	**-0.58**	**-0.48**	**-0.38**
12	**-0.28**	**-0.31**	**-0.26**	-0.17	**-0.30**	**-0.30**	**-0.34**
13	**-0.52**	**-0.41**	**-0.32**	**-0.55**	**-0.49**	**-0.41**	**-0.33**
14	**-0.42**	**-0.30**	-0.07	**-0.43**	**-0.42**	**-0.29**	-0.10
15	**-0.40**	**-0.40**	**-0.26**	**-0.41**	**-0.41**	**-0.37**	**-0.34**
16	**-0.76**	**-0.49**	**-0.27**	**-0.74**	**-0.60**	**-0.68**	**-0.22**
17	**-0.27**	**-0.33**	-0.21	**-0.25**	**-0.45**	**-0.26**	-0.24
18	**0.33**	0.03	**-0.51**	**0.29**	-0.03	**0.32**	**-0.53**
19	**0.66**	-0.09	**-0.35**	**0.63**	-0.11	**0.64**	**-0.34**
20	0.07	-0.26	-0.06	-0.01	**-0.42**	0.14	-0.06

Bold characters denote significant correlation at p=10%.

Table 3. Distribution parameters and goodness-of-fit statistics for selected stations during the DJFMAM season.

	Model	α_0	α_1	α_2	k_0	k_1	k_2	SSE	R^2
Montréal/St-Hubert	Stat.	5.39			1.74			0.0225	0.9867
	Time	5.57	-0.01		1.56	0.01		0.0203	0.9879
	NAO	5.36	-0.13		1.75	0.04		0.0214	0.9872
	PNA	5.36	-0.16		1.73	-0.04		0.0215	0.9873
	Time+NAO	5.49	0.00	-0.09	1.54	0.01	-0.03	0.0200	0.9881
	Time+PNA	5.53	-0.01	-0.15	1.54	0.01	-0.05	**0.0194**	**0.9885**
	NAO+PNA	5.34	-0.12	-0.14	1.74	0.05	-0.05	0.0206	0.9877
Roberval	Stat.	4.64			1.53			0.0339	0.9758
	Time	5.07	-0.01		1.54	0.00		0.0291	0.9778
	NAO	4.58	-0.32		1.53	-0.05		0.0283	0.9789
	PNA	4.62	-0.10		1.53	0.00		0.0335	0.9759
	Time+NAO	4.85	-0.01	-0.23	1.48	0.00	-0.07	**0.0270**	**0.9794**
	Time+PNA	5.05	-0.01	-0.09	1.55	0.00	0.00	0.0288	0.9778
	NAO+PNA	4.57	-0.31	-0.06	1.53	-0.05	0.00	0.0282	0.9789
Québec/Jean Lesage Intl	Stat.	5.23			1.58			0.0418	0.9734
	Time	5.85	-0.02		1.65	0.00		0.0327	0.9776
	NAO	5.14	-0.44		1.58	-0.04		0.0326	0.9788
	PNA	5.18	-0.26		1.57	-0.03		0.0394	0.9748
	Time+NAO	5.58	-0.01	-0.29	1.62	0.00	-0.04	**0.0296**	**0.9800**
	Time+PNA	5.79	-0.02	-0.23	1.64	0.00	-0.04	0.0308	0.9789
	NAO+PNA	5.10	-0.41	-0.19	1.57	-0.04	-0.03	0.0313	0.9796
Mont-Joli	Stat.	6.43			1.80			0.0326	0.9838
	Time	7.03	-0.02		1.83	0.00		0.0253	0.9873
	NAO	6.37	-0.31		1.81	0.00		0.0284	0.9855
	PNA	6.38	-0.24		1.80	-0.03		0.0308	0.9847
	Time+NAO	6.90	-0.01	-0.14	1.84	0.00	0.00	0.0247	0.9875
	Time+PNA	6.97	-0.02	-0.21	1.82	0.00	-0.03	**0.0239**	**0.9880**
	NAO+PNA	6.33	-0.29	-0.19	1.80	0.00	-0.03	0.0273	0.9861
Schefferville	Stat.	5.25			1.63			0.0408	0.9750
	Time	5.71	-0.01		1.50	0.00		0.0346	0.9778
	NAO	5.20	-0.32		1.66	0.06		0.0353	0.9775
	PNA	5.20	-0.20		1.63	-0.01		0.0392	0.9756

	Time+NAO	5.50	-0.01	-0.20	1.51	0.00	0.00	**0.0333**	**0.9785**
	Time+PNA	5.66	-0.01	-0.19	1.50	0.00	-0.02	0.0333	0.9784
	NAO+PNA	5.17	-0.30	-0.13	1.65	0.06	-0.03	0.0346	0.9778
Gaspé	Stat.	3.95			1.34			0.0352	0.9675
	Time	4.29	-0.01		1.25	0.00		0.0312	0.9697
	NAO	3.97	-0.25		1.35	0.00		0.0322	0.9693
	PNA	3.94	-0.12		1.34	-0.03		0.0347	0.9683
	Time+NAO	4.22	-0.01	-0.18	1.25	0.00	-0.03	0.0299	0.9708
	Time+PNA	4.33	-0.02	-0.21	1.26	0.00	-0.01	**0.0298**	**0.9711**
	NAO+PNA	3.96	-0.25	-0.11	1.34	0.00	-0.03	0.0318	0.9699
Natashquan	Stat.	5.50			1.69			0.0403	0.9740
	Time	4.76	0.04		1.49	0.01		0.0252	0.9832
	NAO	5.51	-0.10		1.69	-0.02		0.0400	0.9742
	PNA	5.45	-0.35		1.68	-0.09		0.0355	0.9770
	Time+NAO	4.76	0.04	-0.19	1.49	0.01	-0.04	0.0239	0.9839
	Time+PNA	4.80	0.03	-0.20	1.51	0.01	-0.05	**0.0238**	**0.9840**
	NAO+PNA	5.46	-0.09	-0.34	1.68	-0.02	-0.09	0.0353	0.9771

Bold characters denote the best results for a given station.

Figure captions

Figure 1. Overview of the methodology for wind energy assessment at a given site over a long-term horizon.

Figure 2. Spatial distribution of the meteorological stations.

Figure 3. Average monthly wind speed at the stations of Montréal/St-Hubert and Val-d'Or.

Figure 4. Boxplots of correlation coefficients between the seasonal average of the NAO and PNA indices and the seasonal average wind speed. Dotted lines represent significance limits for a fictive sample of 50 years.

Figure 5. Trends in seasonal covariates of climate indices. 1953-2020 for NAO (DJF) and 1953-1982 and 1983-2020 for PNA (MAM).

Figure 6. Frequency histograms for observed wind speed data during the winter season (DJF) where data are segregated by the positive phase and negative phase of NAO (DJF) at the stations of Mont-Joli and Québec/Jean Lesage Intl. (a, b), and during the spring season (MAM) where data are classified according to the positive and negative phases of PNA (MAM) at the stations of Bagotville and Val-d'Or (c, d). Adjusted W pdfs are superimposed on each graph.

Figure 7. Probability density functions fitted to the observed wind speed data during the winter-spring season (DJFMAM) where data are classified according to the positive and negative phases of NAO (DJF) and PNA (MAM) at the stations of Bagotville (a) and Québec/Jean Lesage Intl. (b).

Figure 8. Boxplots of the goodness-of-fit statistics (DJFMAM season).

Figure 9. Boxplots of the goodness-of-fit statistics (DJF season).

Figure 10. Boxplots of the goodness-of-fit statistics (MAM season).

Figure 11. pdf for each year with the nonstationary model using the covariates Time and NAO for the winter season at Québec/Jean Lesage Intl.

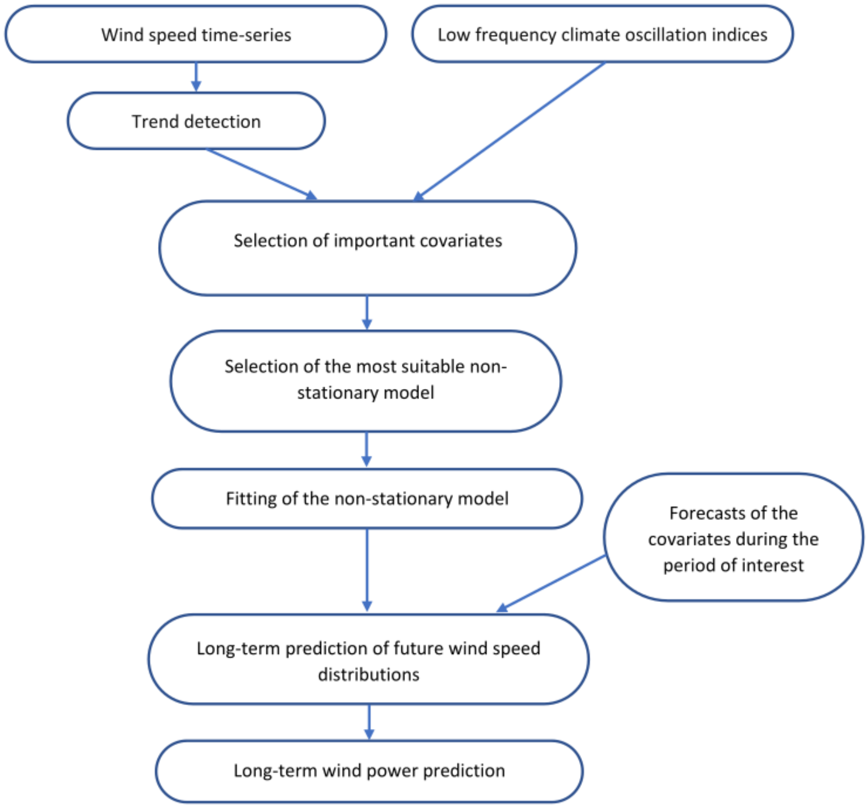
Wind speed time-series
Low frequency climate oscillation indices
Trend detection
Selection of important covariates
Selection of the most suitable non-stationary model
Fitting of the non-stationary model
Forecasts of the covariates during the period of interest
Long-term prediction of future wind speed distributions
Long-term wind power prediction

Figure 1

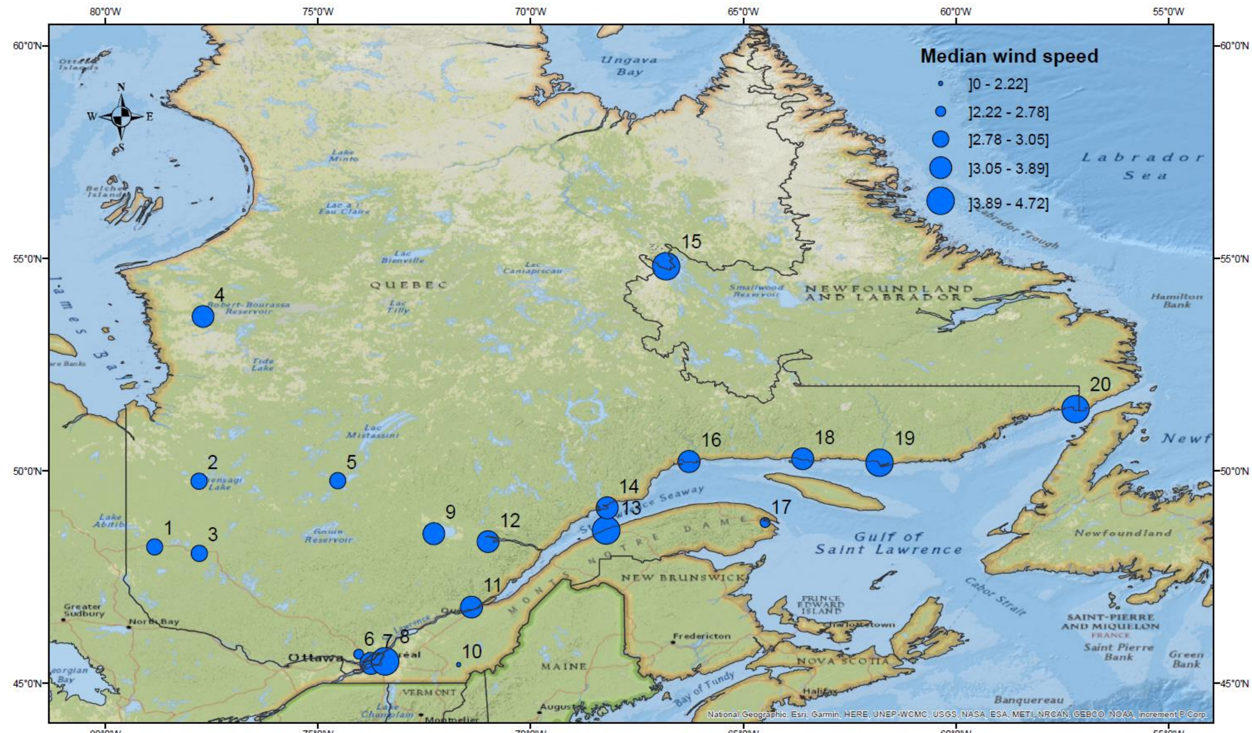
Median wind speed
]0 - 2.22]
]2.22 - 2.78]
]2.78 - 3.05]
]3.05 - 3.89]
]3.89 - 4.72]
80°0'W
75°0'W
70°0'W
65°0'W
60°0'W
55°0'W
60°0'N
55°0'N
50°0'N
45°0'N
1
2
3
4
5
6
7
8
9
10
11
12
13
14
15
16
17
18
19
20
Ungava Bay
Labrador Sea
QUEBEC
NEWFOUNDLAND AND LABRADOR
Gulf of Saint Lawrence
NEW BRUNSWICK
NOVA SCOTIA
MAINE
VERMONT
Ottawa
Newfoundland
Fredericton
Bay of Fundy
National Geographic, Esri, Garmin, HERE, UNEP-WCMC, USGS, NASA, ESA, METI, NRCAN, GEBCO, NOAA, increment P Corp.

Figure 2

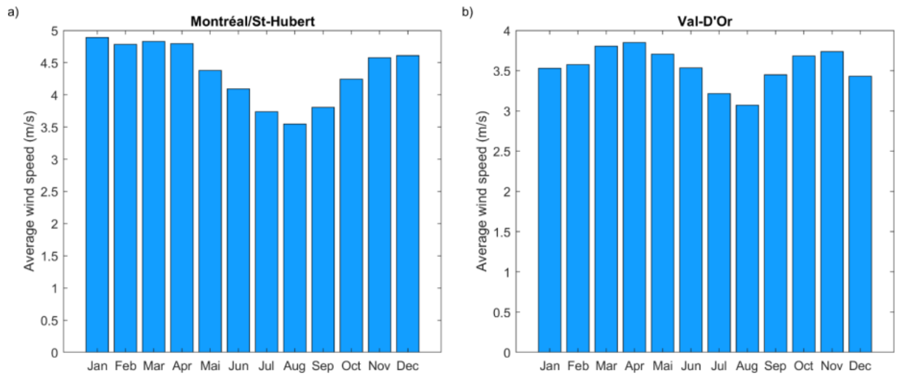
a)
Montréal/St-Hubert
Average wind speed (m/s)
0
0.5
1
1.5
2
2.5
3
3.5
4
4.5
5
Jan Feb Mar Apr Mai Jun Jul Aug Sep Oct Nov Dec
b)
Val-D'Or
Average wind speed (m/s)
0
0.5
1
1.5
2
2.5
3
3.5
4
Jan Feb Mar Apr Mai Jun Jul Aug Sep Oct Nov Dec

Figure 3

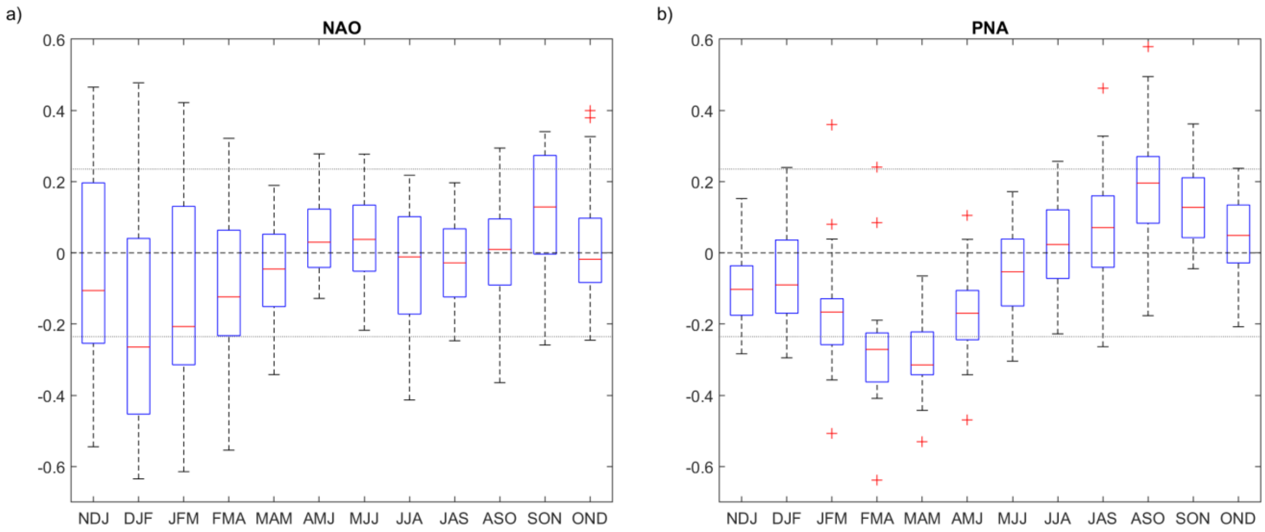

a)
NAO
b)
PNA
0.6
0.4
0.2
0
-0.2
-0.4
-0.6
NDJ DJF JFM FMA MAM AMJ MJJ JJA JAS ASO SON OND

Figure 4

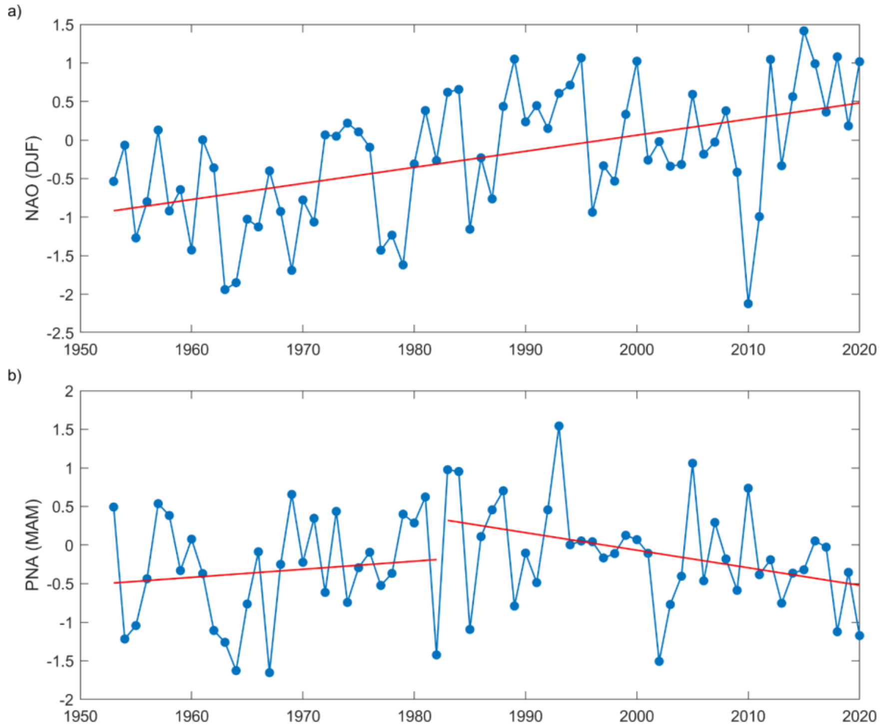

a)
NAO (DJF)
1.5
1
0.5
0
-0.5
-1
-1.5
-2
-2.5
1950
1960
1970
1980
1990
2000
2010
2020
b)
PNA (MAM)
2
1.5
1
0.5
0
-0.5
-1
-1.5
-2
1950
1960
1970
1980
1990
2000
2010
2020

Figure 5

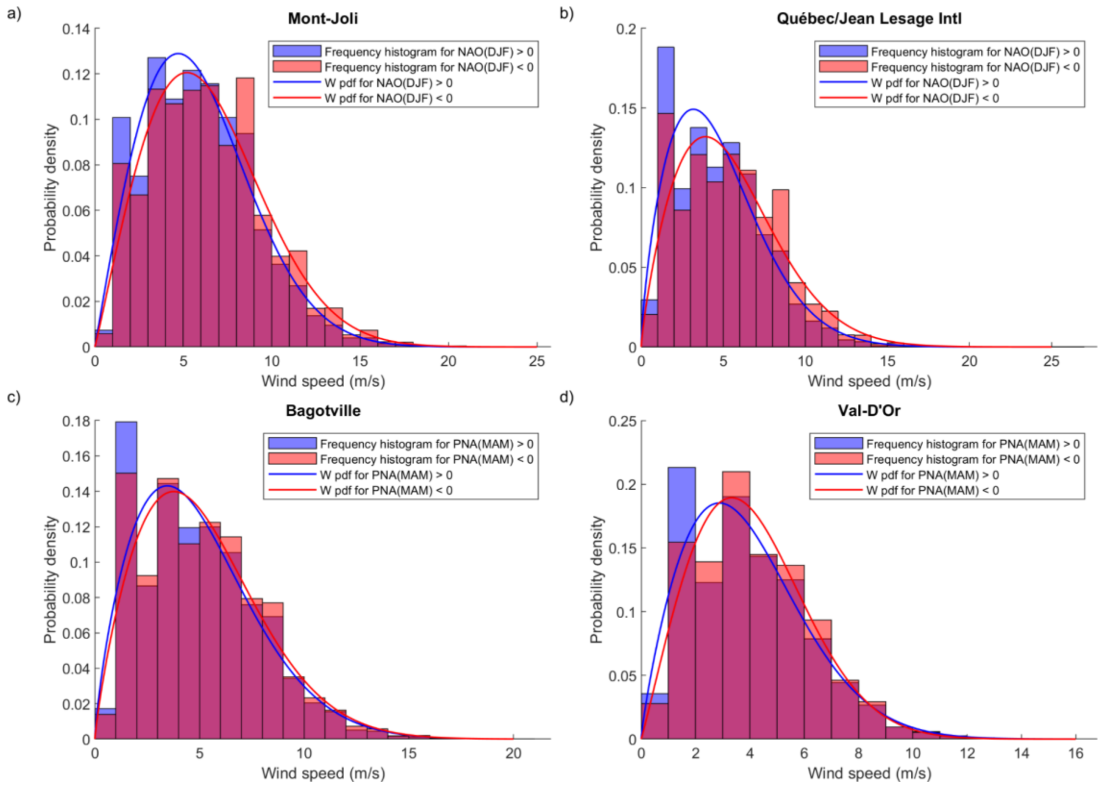
a)
Mont-Joli
b)
Québec/Jean Lesage Intl
c)
Bagotville
d)
Val-D'Or
Frequency histogram for NAO(DJF) > 0
Frequency histogram for NAO(DJF) < 0
W pdf for NAO(DJF) > 0
W pdf for NAO(DJF) < 0
Frequency histogram for PNA(MAM) > 0
Frequency histogram for PNA(MAM) < 0
W pdf for PNA(MAM) > 0
W pdf for PNA(MAM) < 0
Probability density
Wind speed (m/s)

Figure 6

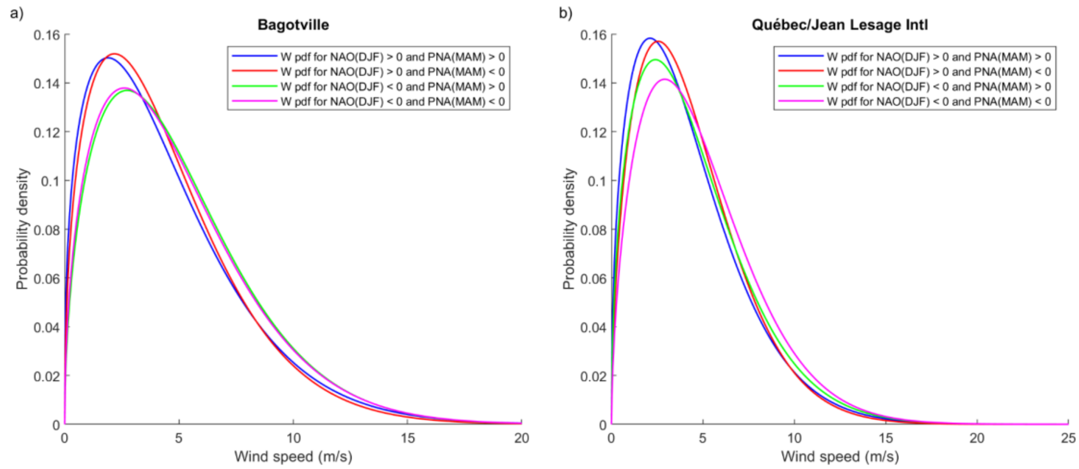
a)
Bagotville
0.16
0.14
0.12
0.1
0.08
0.06
0.04
0.02
0
Probability density
0
5
10
15
20
Wind speed (m/s)
W pdf for NAO(DJF) > 0 and PNA(MAM) > 0
W pdf for NAO(DJF) > 0 and PNA(MAM) < 0
W pdf for NAO(DJF) < 0 and PNA(MAM) > 0
W pdf for NAO(DJF) < 0 and PNA(MAM) < 0
b)
Québec/Jean Lesage Intl
0.16
0.14
0.12
0.1
0.08
0.06
0.04
0.02
0
Probability density
0
5
10
15
20
25
Wind speed (m/s)
W pdf for NAO(DJF) > 0 and PNA(MAM) > 0
W pdf for NAO(DJF) > 0 and PNA(MAM) < 0
W pdf for NAO(DJF) < 0 and PNA(MAM) > 0
W pdf for NAO(DJF) < 0 and PNA(MAM) < 0

Figure 7

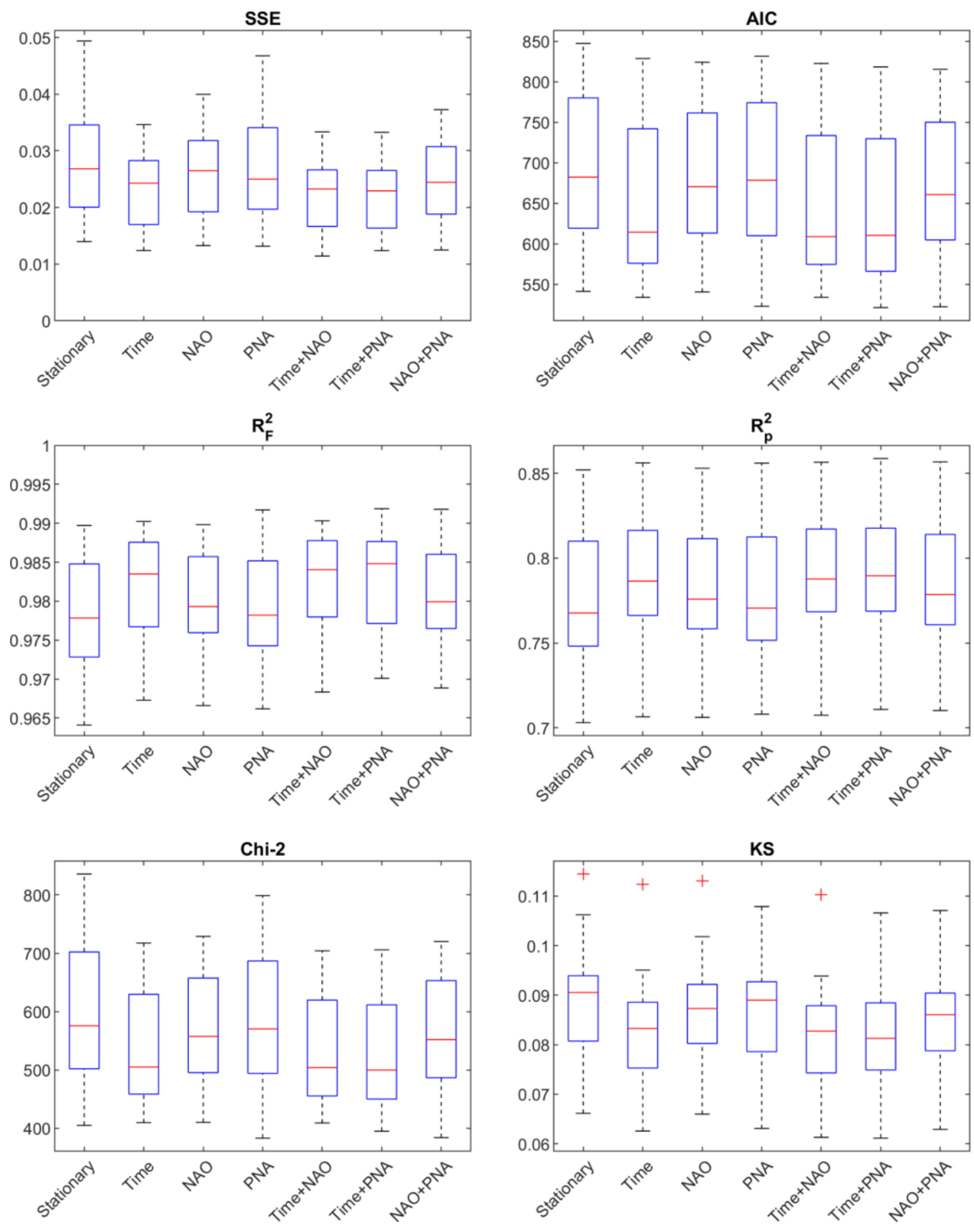
SSE
AIC
R_F^2
R_p^2
Chi-2
KS
Stationary
Time
NAO
PNA
Time+NAO
Time+PNA
NAO+PNA

Figure 8

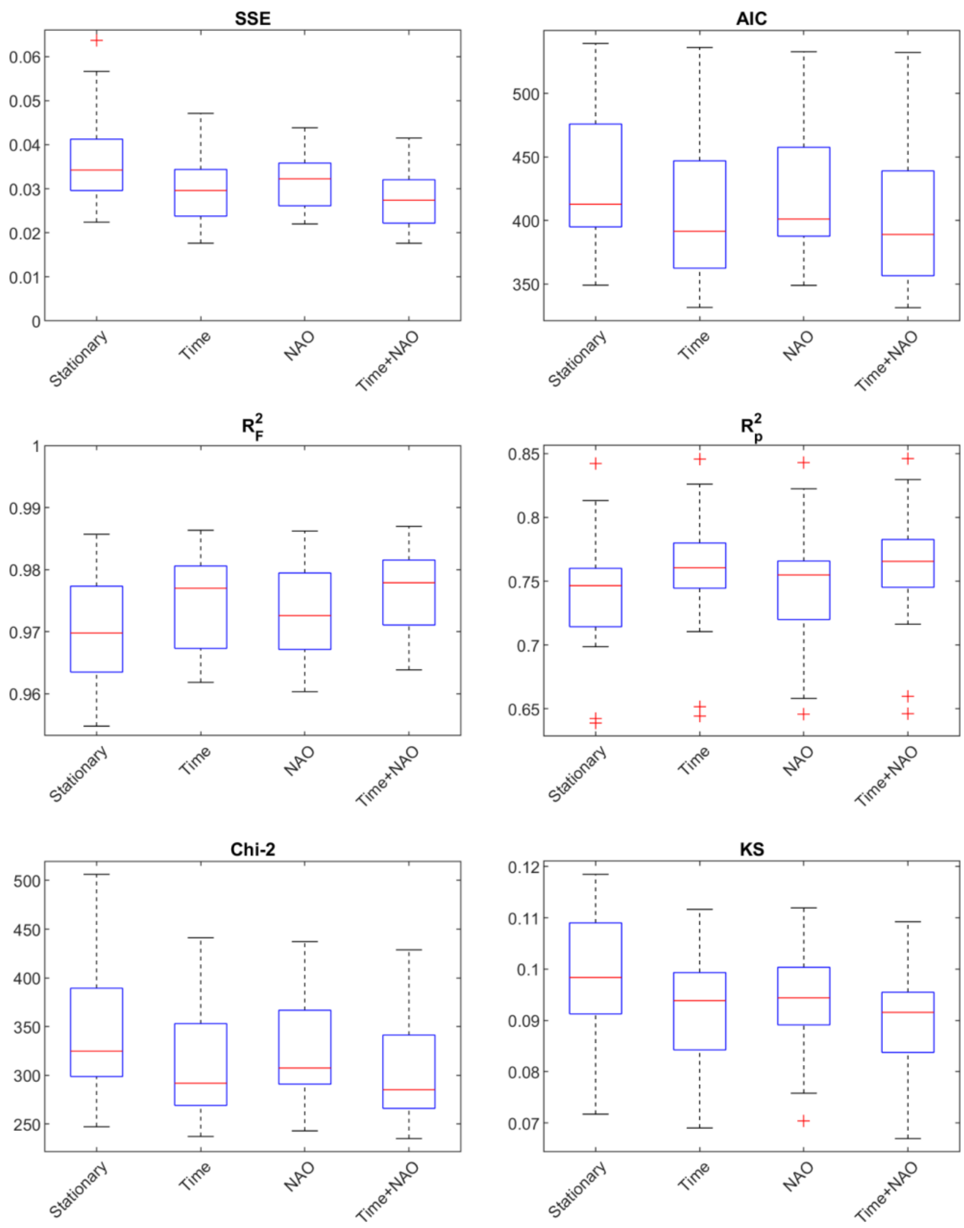
SSE
0.06
0.05
0.04
0.03
0.02
0.01
0
Stationary
Time
NAO
Time+NAO
AIC
500
450
400
350
Stationary
Time
NAO
Time+NAO
R^2_F
1
0.99
0.98
0.97
0.96
Stationary
Time
NAO
Time+NAO
R^2_p
0.85
0.8
0.75
0.7
0.65
Stationary
Time
NAO
Time+NAO
Chi-2
500
450
400
350
300
250
Stationary
Time
NAO
Time+NAO
KS
0.12
0.11
0.1
0.09
0.08
0.07
Stationary
Time
NAO
Time+NAO

Figure 9

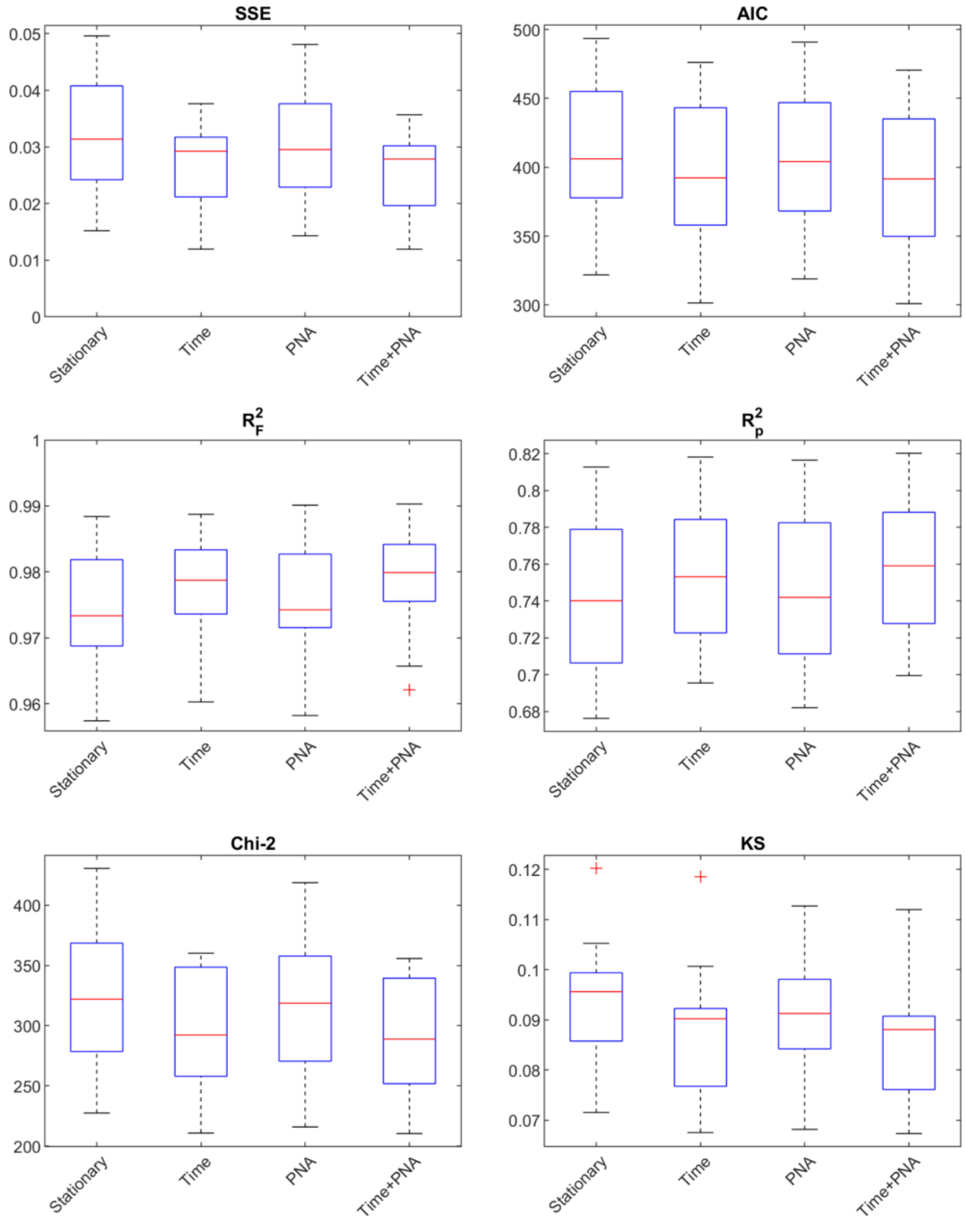

SSE
0.05
0.04
0.03
0.02
0.01
0
Stationary
Time
PNA
Time+PNA
AIC
500
450
400
350
300
R_F^2
1
0.99
0.98
0.97
0.96
R_p^2
0.82
0.8
0.78
0.76
0.74
0.72
0.7
0.68
Chi-2
400
350
300
250
200
KS
0.12
0.11
0.1
0.09
0.08
0.07

Figure 10

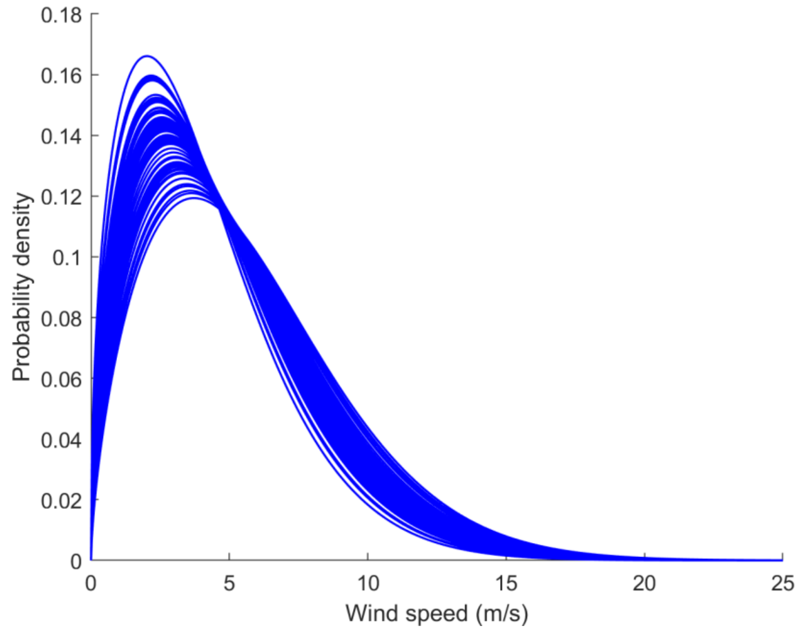
0.18
0.16
0.14
0.12
0.1
0.08
0.06
0.04
0.02
0
Probability density
0
5
10
15
20
25
Wind speed (m/s)

Figure 11